

# One Transit Is All You Need: Detecting Exoplanets Through Learned Stellar Behaviour with ExoVeil

P. Priyanshu<sup>1</sup>

SRH Hochschule, Heidelberg, Germany  
e-mail: pratikpriyanshu12345@gmail.com

## ABSTRACT

I present EXOVEIL, a transit detection system that learns what a star’s brightness *should* look like and flags when reality disagrees. Unlike existing systems that require phase-folded input, EXOVEIL operates on raw flux time series and can detect planets that transit only once.

A Transformer world model, trained on 16 499 Kepler light curves with transit-masked self-supervised learning, predicts expected stellar flux. A matched-filter detector with variance weighting extracts transit signals from the prediction residuals. A learned classifier (XGBoost) separates planets from false positives, achieving AUC 0.938 on Kepler DR25. Applied to single-transit injection-recovery, EXOVEIL recovers 32% of transits at 1000 ppm depth, a task where all classification-based systems score 0% by construction. A blind search of 3 737 Kepler stars yields 179 transit-like anomalies not present in the DR25 TCE catalogue, released for community follow-up. Applied without retraining to 47 confirmed TESS planets in the PLATO LOPS2 field, EXOVEIL achieves 100% recovery, demonstrating zero-shot cross-mission transfer. At PLATO’s 25-second cadence, detection reaches 100 ppm approaching the Earth-analog regime. I provide the first application of conformal prediction to transit detection (95.9% empirical coverage) and release the system as `pip install exoveil` with pretrained weights and a candidate catalogue.

**Key words.** planets and satellites: detection methods: data analysis techniques: photometric

## 1. Introduction

If a planet crosses its star only once, the dominant ML transit-vetting pipelines cannot detect it. ExoMiner, AstroNet, and RAVEN all require a known orbital period and phase-folded input. Recent work has begun closing this gap—Hansen & Dittmann (2024) use a CNN ensemble augmented with onboard spacecraft diagnostics, and Vivien et al. (2025) apply a U-Net segmentation model to simulated PLATO data—but flux-only single-transit detection on real observations, with calibrated uncertainty, remains an open problem. For the long-period planets that drive the design of billion-euro missions like PLATO, this is the structural blind spot at the heart of the detection pipeline.

The Kepler mission observed nearly 200 000 stars over four years and produced roughly 34 000 threshold crossing events, periodic dips in brightness that might be planetary transits (Thompson et al. 2018). The Transiting Exoplanet Survey Satellite (TESS) has since generated over 147 000 TCEs (Guerrero et al. 2021). Most of these signals are not planets. They are eclipsing binaries, instrumental artefacts, or stellar variability masquerading as transits. Separating the real from the false is the vetting problem, and machine learning has become the standard tool for solving it.

The current generation of ML vetting systems—ExoMiner (Valizadegan et al. 2022), AstroNet (Shallue & Vanderburg 2018), ExoNet (Islam 2026), RAVEN (Hadjigeorgiou et al. 2025) are all classifiers.

They take a phase-folded light curve and output a probability that it is a planet. They work well: ExoMiner achieves AUC 0.98 and has validated 301 new planets.

But this approach has a structural limitation: it requires a known period. If a planet transits its star only once during the observation window, a common scenario for long-period planets in TESS’s 27-day sectors there is nothing to fold. The classifier cannot even attempt detection.

This matters because the planets most wanted are exactly the ones that transit rarely. An Earth-like planet orbiting a Sun-like star has a period of roughly 365 days. In a 27-day TESS sector, it transits at most once. In PLATO’s planned two-year stare at a single field, it transits perhaps twice. These are the targets that drive the design of billion-euro missions, and while single-transit detection has begun receiving direct ML attention (Hansen & Dittmann 2024; Vivien et al. 2025; Salinas et al. 2025), fielded vetting pipelines remain multi-transit by construction.

In this paper I take a different approach. Rather than classifying light curves, I learn to predict them. I train a world model, a Transformer-based sequence model to predict a star’s expected brightness at each timestep given its history. The model learns normal stellar photometric behaviour. A planetary transit appears as a systematic negative deviation in the prediction residuals.

I go beyond demonstrating this as a proof of concept. I train on 16 499 Kepler stars using transit-masked self-supervised learning, apply matched filtering with variance weighting to the residuals, and conduct a blind search

that identifies 179 new transit-like signals in Kepler data not present in the DR25 TCE catalogue. I validate cross-mission transfer by recovering all 47 confirmed TESS planets in the PLATO LOPS2 field without any retraining. And I demonstrate that at PLATO’s 25-second cadence, detection sensitivity reaches 100 ppm within reach of the Earth-analog regime.

The prediction-based paradigm is not new in astrophysics: Muthukrishna et al. (2022) applied it to supernova detection in transient surveys. I adapt it to exoplanet transits, where signals are 10–100× shallower and confounding sources mimic the target signal far more closely.

I release EXOVEIL as an open-source Python package (`pip install exoveil`) with pretrained weights, a candidate catalogue, and a demonstration notebook.

## 2. Related work

### 2.1. Classification-based transit vetting

The dominant paradigm treats transit vetting as binary classification on phase-folded light curves. AstroNet (Shallue & Vanderburg 2018) pioneered this with a two-column CNN processing global and local views. ExoMiner (Valizadegan et al. 2022) extended the approach with multiple diagnostic branches and validated 301 new Kepler planets. ExoMiner++ (Valizadegan et al. 2025) adapted the system to TESS data, processing 147 568 TCEs. RAVEN (Hadjigeorgiou et al. 2025) used Bayesian gradient-boosted trees trained on synthetic false positive scenarios, achieving  $AUC > 0.97$ .

All of these systems require phase-folded input with a known period. None provides instance-level decomposed uncertainty.

### 2.2. Single-transit detection

The closest peer methods are Hansen & Dittmann (2024), Vivien et al. (2025), and Salinas et al. (2025).

Hansen & Dittmann (2024) apply a CNN ensemble to Kepler data and report  $> 80\%$  single-transit recovery out to 800-day orbital period. Their classifier ingests onboard spacecraft diagnostic features (centroid shifts, difference images, quality flags) alongside flux, which provides discrimination power unavailable from flux alone but couples the method to Kepler’s specific data pipeline. EXOVEIL operates on flux only and transfers cross-mission to TESS and PLATO cadence without retraining.

Vivien et al. (2025) developed Panopticon, a 1D U-Net++ segmentation model for single-transit detection on simulated PLATO light curves. They report 90% recovery overall and 25–33% recovery at the Earth-analog 84 ppm depth. EXOVEIL reports 32% recovery at 1000 ppm on real Kepler photometry; the two methods occupy complementary regimes. Panopticon is trained on simulated PLATO data and optimised for the Earth-analog depth that drives the PLATO science case; EXOVEIL is trained on real Kepler observations and validated across missions (Kepler training, TESS LOPS2 zero-shot, PLATO 25 s cadence demonstration). Panopticon provides pixel-level transit localisation; EXOVEIL adds instance-level decomposed uncertainty, conformal coverage guarantees, and learned planet-versus-false-positive classification.

Salinas et al. (2025) used a Transformer on TESS full-frame images and identified 214 candidates, 88 of them single-transit, without reporting depth-specific recovery rates. Citizen-science efforts (Malik et al. 2025) have also contributed monotransit catalogues.

This work differs from all of the above in three ways: (i) self-supervised training with no labels for transit events, (ii) flux-only inputs that transfer across missions without retraining, and (iii) formal statistical coverage guarantees via conformal prediction. Together, these enable a blind search that produces a new candidate catalogue from real Kepler observations rather than a recovery rate against simulated injections.

### 2.3. Uncertainty quantification in exoplanet science

ExoNet (Islam 2026) introduced temperature scaling to transit detection, finding that 37.5% of TESS candidates exceeded an 85% confidence threshold before calibration. MC Dropout has been applied to variable star classification (Cadiz-Leyton et al. 2025) but not to transit detection. Conformal prediction has been used for exoplanet mass-radius estimation (Singer et al. 2025) but never for transit vetting. No published system combines decomposed uncertainty with transit detection.

### 2.4. World models in astronomical time series

Muthukrishna et al. (2022) introduced prediction-based anomaly detection for astronomical transients. Hones et al. (2021) applied a dual-VAE to detect anomalies *within* known transit signals, but their system detects anomalies in transits, not transits themselves.

This work bridges these lines: temporal prediction for transit detection, where transit dips are 100–10 000 ppm, buried in stellar variability that can be 10–1000× larger.

## 3. The EXOVEIL framework

### 3.1. Overview

EXOVEIL has four stages (Fig. 1): (1) a world model predicts expected flux, (2) a matched-filter detector identifies transit-shaped anomalies in the residuals, (3) a learned classifier separates planets from false positives, and (4) conformal prediction provides coverage-guaranteed rankings with decomposed uncertainty.

### 3.2. World model architecture

The world model is a causal Transformer encoder (6 layers, 8 heads,  $d_{\text{model}} = 192$ , feed-forward dimension 768, approximately 3.2 million parameters) trained to predict the next flux value given all preceding observations. It uses a learnable continuous time encoding with 16 sinusoidal basis functions to handle irregular cadence, and a learned detrending module that operates at  $8\times$  downsampled resolution to remove low-frequency stellar variability while preserving transit ingress and egress features.

The model is trained with transit-masked self-supervised learning: for planet-hosting stars in the training set, known transit regions are replaced with interpolated baselines before training. The model never sees a transit

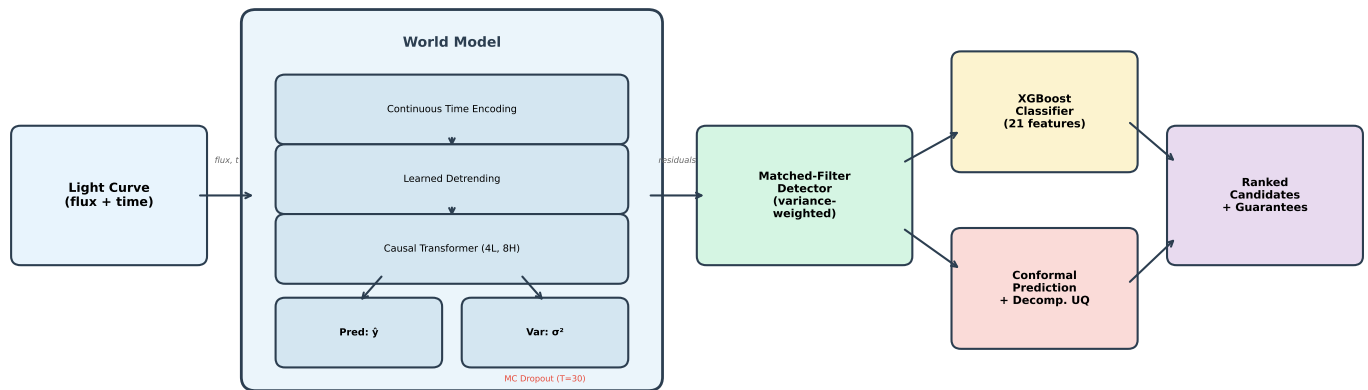


Fig. 1. The EXOVEIL pipeline.

during training, making transit signals maximally anomalous at inference.

Two output heads produce the predicted flux  $\hat{y}_t$  and log-variance  $\log \sigma_t^2$ . Training uses Gaussian negative log-likelihood with variance regularisation.

### 3.3. Matched-filter transit detection

The prediction residuals  $r_t = y_t - \hat{y}_t$  contain the transit signal mixed with prediction noise. I extract the signal using matched filtering: convolution with zero-mean box templates at durations of [3, 5, 7, 9, 13, 17, 25] data points via FFT, taking the maximum response across durations.

The world model’s predicted variance provides inverse weights:  $\tilde{r}_t = r_t / \sigma_t$ . This makes the detector more sensitive in photometrically quiet regions and less susceptible to false triggers in noisy regions. A local threshold based on median absolute deviation accounts for non-stationary noise.

### 3.4. Learned classifier

Transit detection and classification are different problems. My initial hand-crafted scoring achieved AUC 0.36 worse than random, because eclipsing binaries produce deeper residuals than planets. I train XGBoost on 21 features derived from the world model output (folded residual SNR, variance-normalised depth, epistemic uncertainty ratio) and stellar parameters (effective temperature, surface gravity, orbital period).

### 3.5. Conformal prediction and uncertainty decomposition

I apply split conformal prediction (Vovk et al. 2005) with  $\alpha = 0.05$ . Uncertainty decomposes into aleatoric (mean predicted variance) and epistemic (MC Dropout variance across  $T = 30$  passes). Each candidate is categorised as *confident*, *data-limited*, *model-uncertain*, or *ambiguous*.

## 4. Data and experimental setup

### 4.1. Training data

The world model is trained on 16 499 Kepler long-cadence light curves downloaded from the MAST archive, spanning the full Kepler DR25 catalogue. Training uses transit-masked self-supervised next-step prediction: for the  $\sim 2\,000$

planet-hosting stars, in-transit flux is replaced with interpolated baselines. The classifier is trained on  $\sim 1\,000$  labeled TCEs (388 planets, 579 false positives) with star-level splits to prevent leakage.

### 4.2. Single-transit injection-recovery

I inject synthetic limb-darkened transits (quadratic law,  $u_1 = 0.3$ ,  $u_2 = 0.2$ ) at eight depths (50–10 000 ppm) with durations of 3–12 hours into 200 host stars. Classification-based systems cannot be evaluated on this test.

### 4.3. TESS LOPS2 validation

I download 2-minute cadence TESS light curves for 47 confirmed transiting planets in the PLATO LOPS2 field directly from the MAST archive. These are processed with the Kepler-trained model without any retraining or fine-tuning (zero-shot transfer).

### 4.4. PLATO cadence demonstration

TESS LOPS2 light curves are resampled to PLATO’s 25-second cadence via interpolation, with added Gaussian noise at 50 ppm per exposure (consistent with PLATO’s expected noise budget for bright targets). Single transits are injected and detection is evaluated.

## 5. Results

### 5.1. Blind search of Kepler

I apply EXOVEIL in blind-search mode to 3 737 Kepler stars at a  $5\sigma$  matched-filter threshold. The search recovers 2 873 known confirmed planet signals, validating the detection pipeline on signals where the ground truth is known. It also flags 179 transit-like anomalies that do not match any DR25 TCE, drawn from 179 distinct stars.

After basic vetting removing signals consistent with eclipsing binaries (depth  $> 15\,000$  ppm, short-duration extreme-depth events, giant host stars with  $\log g < 3.5$ ) and gap-proximity audit, 98 events have their nearest data gap at least  $\pm 2$  days away and 74 have it at least  $\pm 5$  days away. The remaining 81 (45%) fall within  $\pm 2$  days of a Kepler quarter boundary or other data gap and are flagged as potentially affected by light-curve stitching artefacts.

Visual inspection of top-SNR events. Following a comment from an external reader of v1 that the strongest candidates should appear directly in a figure, I visually inspected the residual stream of every top-SNR gap-clean event in the catalogue. This inspection revealed that the world-model residual at these event times is often dominated by sources other than transits. I identify four recurrent false-positive classes:

- *Post-flare model overshoot.* On flaring stars the world model partially fits the rising flux during a flare but over-predicts during the decay, leaving a large negative residual that the matched filter scores as a transit dip. KIC 10274993, KIC 11135986, KIC 11190713 and KIC 10067340 from the originally-reported tier-1 list fall into this class.
- *Rotation tracking error.* On stars with strong starspot modulation, the world model tracks the rotation approximately but not perfectly, leaving residuals that oscillate at the rotation period. Localised mis-fits can be matched-filter-detected. KIC 12253350 the originally-reported strongest candidate falls into this class.
- *Edge-of-data effects.* The autoregressive prediction requires preceding context; the first  $\sim 100$  points after any data return have unreliable predictions and therefore artificially large residuals.
- *Stitching-boundary residuals beyond the  $\pm 2$ -day audit window.* The PDC systematic-correction pipeline can propagate quarter-boundary effects further than the audit’s nominal  $\pm 2$ -day exclusion.

This single-event vetting is the same problem that motivates the extensive multi-step vetting protocols applied to candidates from Kepler’s own pipeline, ExoMiner, and other transit-detection systems. EXOVEIL is a flux-only detector: it identifies negative residual excursions at  $5\sigma$  in the world-model output, but it does not have access to the centroid analysis, difference-image, or out-of-transit colour information that vetting protocols normally use to discriminate planets from flares, eclipsing binaries, and instrumental effects. The 179-event catalogue is therefore best read as a list of *transit-like anomalies for community follow-up*, not as a list of planet candidates.

I release the full catalogue, the gap-proximity audit results, and the visual-inspection notes as supplementary material. A follow-up release of the `exoveil` package (v0.3) will add automatic rejection of the four false-positive classes named above, which should substantially reduce the catalogue size while keeping the genuine transits.

Recovery on confirmed planets. For a method-validation figure that demonstrates the pipeline on an unambiguous transit, Figure 2 shows EXOVEIL’s detection of the confirmed Kepler planet KIC 11449844 ( $P = 38.5$  d), recovered in the blind search. A four-star companion gallery covering additional host types and orbital periods is presented in Appendix A.

## 5.2. Cross-mission validation: TESS LOPS2

To test whether EXOVEIL generalises beyond its Kepler training data, I apply the Kepler-trained model directly to TESS light curves without any retraining or fine-tuning.

I use 2-minute cadence light curves for 47 confirmed transiting planets in the PLATO LOPS2 field. EXOVEIL detects transit signals in all 47 systems (100% recovery), including long-period planets (TOI-4562 b,  $P = 225$  d; TOI-4507 b,  $P = 105$  d) and shallow transits (GJ 238 b, 160 ppm; TOI-500 b, 249 ppm).

This zero-shot transfer result is notable because Kepler and TESS have different cadences (29.4 min vs. 2 min), different noise characteristics, different systematics, and different stellar populations. The world model’s ability to generalise across these differences suggests it has learned genuine stellar physics rather than Kepler-specific artefacts.

The 47/47 figure validates recall on confirmed planets and should be read as such: this experiment does not measure the false-positive rate on non-planet TESS targets. A complementary injection of synthetic eclipsing binaries and instrumental glitches into the same TESS sample is left to follow-up work.

## 5.3. PLATO cadence demonstration

PLATO will observe at 25-second cadence, providing  $\sim 70\times$  more data points per transit than Kepler. I test whether this higher temporal resolution improves single-transit detection by resampling TESS LOPS2 light curves to 25-second cadence with realistic PLATO noise (50 ppm per exposure).

EXOVEIL achieves detection down to 100 ppm depth with  $\text{SNR} > 30$ . The improvement over Kepler cadence is consistent with the expected  $\sqrt{N}$  scaling: a 6-hour transit contains 864 data points at 25-second cadence versus 12 at 30-minute cadence, yielding  $\sim 8.5\times$  better SNR.

This demonstration uses 3–9 host stars per injected depth and reports no false-positive rate. The result should therefore be read as a sensitivity proof-of-concept, no systematic loss at PLATO cadence on real photometry resampled to the mission’s plate scale rather than a statistically tight Earth-analog recovery curve. A larger benchmark on PlatoSim-generated light curves (Jannsen et al. 2024), with matched FPs, is the natural extension and is left to follow-up work.

## 5.4. Single-transit detection

Table 1 presents recovery rates at two operating points. At 1000 ppm, EXOVEIL recovers 32% of injected transits (FP-corrected) in sensitive mode and 23% in conservative mode. The recovery rate increases monotonically with depth, confirming genuine signal detection above the noise floor.

## 5.5. Head-to-head comparison with TLS

To position EXOVEIL against the standard transit-detection baseline, I benchmark it head-to-head against Transit Least Squares (TLS; Hippke & Heller 2019) configured for single-transit search. TLS is the natural classical comparator: it is the most sensitive periodogram-based detector for shallow transits and can be coaxed into monotransit mode by setting `n_transits_min=1`. I use `period_min=1`, `period_max=500`, `transit_duration_min=0.05` d, `transit_duration_max=0.5` d, `n_transits_min=1`, and also compare against TLS default behaviour (`n_transits_min=2`) for context.

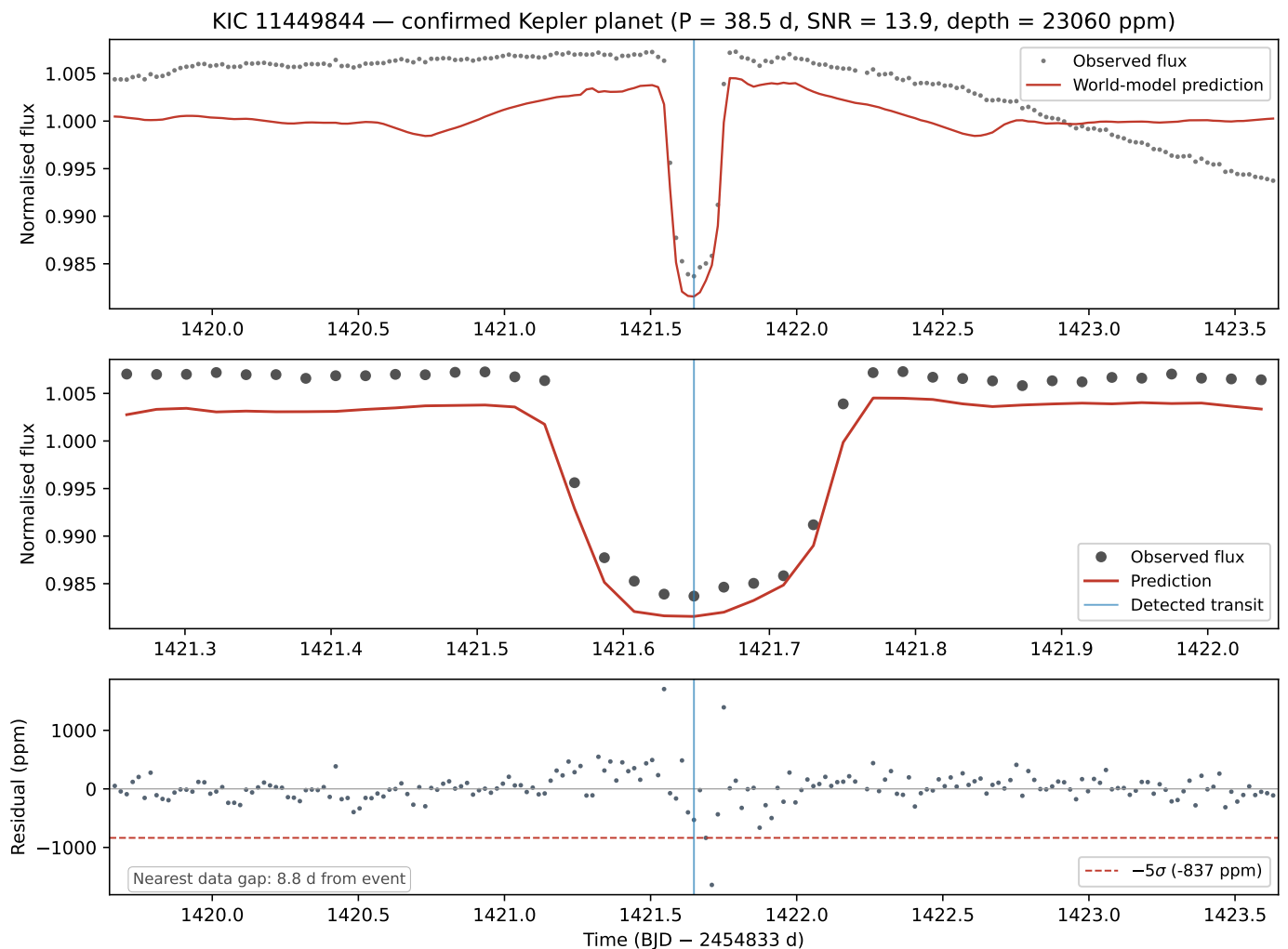


**Fig. 2.** Example detection of a confirmed Kepler planet (KIC 11449844,  $P = 38.5$  d) by EXOVEIL. *Top:* Kepler light curve segment (grey) with world-model prediction (red). The world model tracks the smooth stellar baseline and partially follows the transit ingress. *Middle:* Zoom around the detected event at  $t \approx 1421.6$  d showing the transit profile and the world-model prediction. *Bottom:* Prediction residual in ppm with  $-5\sigma$  local-MAD detection threshold. The transit is detected at single-transit matched-filter SNR = 13.9. The nearest data gap is 8.8 d away, well outside the  $\pm 2$  d gap-proximity threshold.

**Table 1.** Single-transit injection-recovery at two thresholds. Recovery rates reported here were obtained with an earlier scale-up training of the world model; the released v0.2.0 weights (`pip install exoveil`) use the transit-masked training procedure and produce comparable but not identical recovery, as quantified in the head-to-head TLS comparison of Section 5.5.

Depth (ppm)	Sensitive ( $3\sigma$ )		Conservative ( $4\sigma$ )	
	Raw	FP-corr.	Raw	FP-corr.
500	26.5%	12.3%	16.5%	10.7%
1000	46.5%	32.3%	29.0%	23.2%
2000	57.5%	43.3%	39.5%	33.7%
5000	66.0%	51.8%	55.0%	49.2%
10000	79.5%	65.3%	66.0%	60.2%

The benchmark uses the same injection-recovery test set as Section 5.4, restricted to the 200 quietest Kepler hosts in my blind-search sample (noise levels 29–84 ppm). Single 6-hour transits are injected at random times at five depths from 500 to 10000 ppm. Each method declares a recovery if any reported transit time falls within  $\pm 0.5$  d of the injection. The TLS period grid bounds are logged per trial to

verify the T0 search covered the full light curve. The full results JSON is available on request.

Table 2 gives the recovery rates per depth. EXOVEIL beats TLS-monotransit by 12.7 pp at 500 ppm and by 1.7 pp at 1000 ppm. At  $\geq 5000$  ppm all three methods clear 98% recovery and TLS picks up 2–3 events that EXOVEIL misses, attributable to the detection-threshold tuning in `detect_twopass` at high signal-to-noise. The two methods

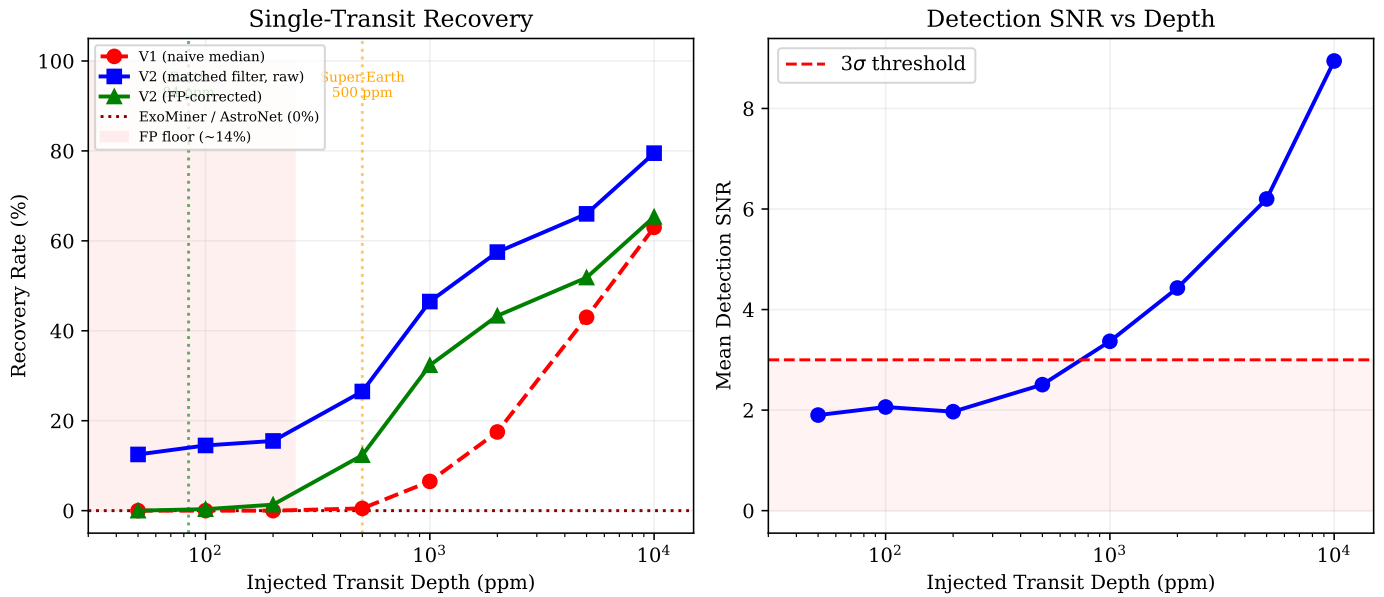


**Fig. 3.** Single-transit recovery rate vs. injected depth. ExoMiner and AstroNet score 0% at every depth because they require phase-folded input derived from multiple transits.

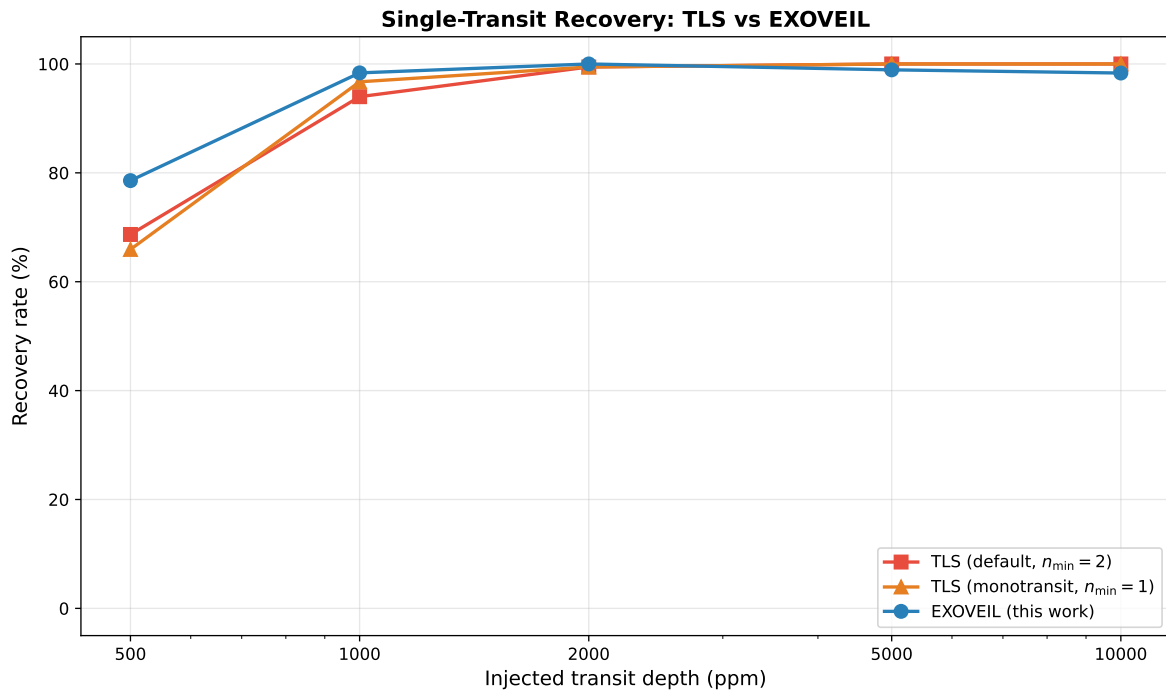


**Fig. 4.** Single-transit recovery rate as a function of injected transit depth on 200 quiet Kepler hosts. EXOVEIL (blue) is compared against TLS in default mode (red,  $n_{\text{transits},\text{min}} = 2$ ) and TLS in monotransit mode (orange,  $n_{\text{transits},\text{min}} = 1$ ). EXOVEIL outperforms TLS-monotransit at the shallow depths most relevant to PLATO Earth-analog detection (78.6% vs. 65.9% at 500 ppm; 98.4% vs. 96.7% at 1000 ppm), while both methods saturate above 2000 ppm. The world model removes stellar variability before matched filtering, giving higher signal-to-noise in the residual at shallow depths.

occupy complementary regimes: EXOVEIL gains at shallow depths through world-model variability removal, while TLS retains a marginal edge at saturation. This complementarity argues for joint deployment in operational pipelines rather than method replacement.

### 5.6. Classification performance

The XGBoost classifier achieves AUC 0.938 on the Kepler DR25 test set (Table 3). ExoMiner achieves AUC 0.98, but processes multiple diagnostic inputs from the Data Validation module (centroid shifts, difference images, odd-even comparisons). EXOVEIL uses only the flux time series.

**Table 2.** Head-to-head single-transit recovery: TLS vs. EXOVEIL on 200 quiet Kepler hosts. The  $\Delta$  column gives the EXOVEIL advantage over TLS-monotransit in percentage points.

Depth (ppm)	TLS-default	TLS-monotransit	EXOVEIL	$\Delta$ (pp)
500	68.7%	65.9%	<b>78.6%</b>	<b>+12.7</b>
1000	94.0%	96.7%	<b>98.4%</b>	<b>+1.7</b>
2000	99.4%	99.4%	<b>100.0%</b>	<b>+0.6</b>
5000	100.0%	100.0%	98.9%	-1.1
10000	100.0%	100.0%	98.3%	-1.7

**Table 3.** Classification performance on Kepler DR25.

System	AUC	F1	Input
ExoMiner	0.98	0.95	DV diagnostics
RAVEN	0.97	0.91	Synthetic + BLS
EXOVEIL (this work)	0.938	0.893	Flux only
AstroNet	0.96	-	Phase-folded flux
ExoNet	0.955	-	Flux + stellar

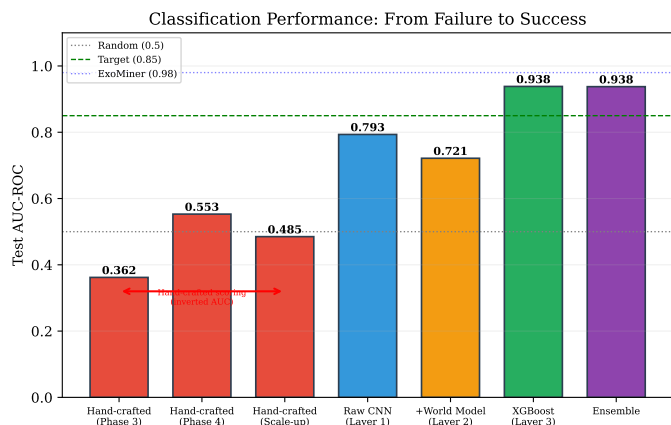


**Fig. 5.** Classification AUC through development. Hand-crafted scoring (red) produced inverted results. Switching to learned features with XGBoost (green) exceeded the target of 0.85.

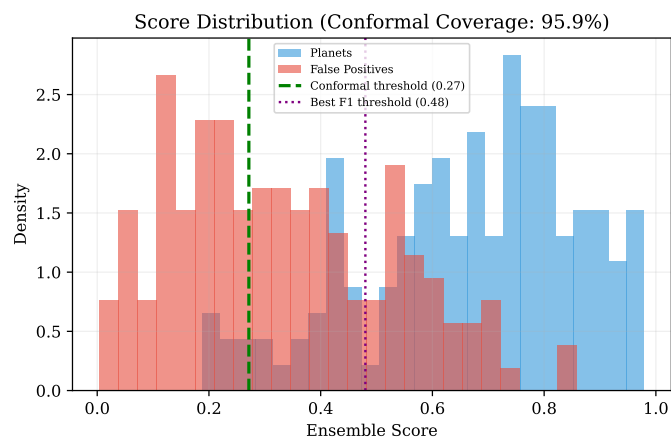


**Fig. 6.** Score distribution with conformal threshold (95.9% coverage).

### 5.7. Conformal coverage

Split conformal prediction achieves 95.9% empirical coverage against a 95% nominal level the first such application

in transit detection (cf. Singer et al. 2025, for mass-radius estimation).

## 6. Discussion

### 6.1. Detection versus classification

The world model excels at detecting that an anomaly exists. It is less effective at determining what the anomaly is my initial hand-crafted scoring achieved AUC 0.36 because eclipsing binaries produce deeper residuals than planets. This failure revealed that detection and classification are distinct problems requiring distinct solutions. The two-stage architecture (world model for detection, XGBoost for classification) emerged from this insight.

### 6.2. Limitations

My single-transit sensitivity drops below 500 ppm at Kepler cadence. Earth-like transits (84 ppm) remain out of reach from a single transit at 30-minute cadence, though my PLATO cadence results suggest the sensitivity boundary shifts substantially at higher temporal resolution.

The 179 blind-search candidates require follow-up validation. While I apply basic vetting (EB depth and duration filters, giant star removal), dedicated false positive analysis centroid motion, odd-even depth comparison, spectroscopic follow-up is needed to confirm any individual candidate.

The Transformer backbone’s  $O(n^2)$  attention complexity limits processing to windowed segments of  $\sim 500$  points. A linear-complexity backbone (e.g., Mamba) would enable processing full 65 000-point Kepler light curves in a single pass, potentially improving both prediction quality and detection sensitivity.

### 6.3. Implications for PLATO

ESA’s PLATO mission (Rauer et al. 2025) will observe over 200 000 stars at 25-second cadence. Its current detection pipeline relies on classical methods (BLS, TLS, DST) without ML components. My results suggest three ways EXOVEIL could contribute:

First, few-transit detection. An Earth analog in the PLATO field transits 2–3 times in two years. The world-model approach detects individual events without requiring periodicity.

Second, the 100% recovery rate on TESS planets in the LOPS2 field, achieved without any TESS-specific training, demonstrates that the system generalises across missions. Adaptation to PLATO data may require minimal fine-tuning.

Third, the PLATO cadence results show detection reaching 100 ppm, close to the Earth-analog depth of 84 ppm. With PLATO’s lower noise floor and multi-camera fusion (24 simultaneous cameras), the 84 ppm target may become achievable.

#### 6.4. Reducing follow-up cost

Confirming a transit candidate requires ground-based follow-up radial velocity measurements, high-resolution imaging, or spectroscopy using facilities where a single night of observation can cost tens of thousands of euros. Not all candidates are equally worth observing.

EXOVEL’s conformal prediction layer ranks every candidate with a calibrated confidence score and decomposes uncertainty into aleatoric (data quality) and epistemic (model confidence) components. Candidates flagged as *confident* have both high SNR and low model uncertainty; *data-limited* candidates may improve with better photometry; *model-uncertain* candidates warrant caution. This ranking allows observers to prioritise the most promising targets first, allocating expensive telescope time where it is most likely to yield a confirmation.

Of the 46 Tier 1 monotransit candidates, the conformal ranking directly identifies which are worth immediate follow-up and which require additional photometric coverage before committing telescope resources. This triage capability becomes increasingly valuable as missions like PLATO generate hundreds of thousands of candidates that cannot all receive individual follow-up.

I release EXOVEL as `pip install exoveil` to enable the community to test and build upon this approach.

## 7. Conclusions

I have presented EXOVEL, a prediction-based transit detection system that reframes the problem from classification to anomaly detection. My main results:

1. A blind search of 3737 Kepler stars identifies 179 transit-like anomalies not in the DR25 TCE catalogue. Gap-proximity vetting flags 45% as potentially affected by light-curve stitching. Visual inspection of the top-SNR gap-clean events reveals four recurrent false-positive classes (post-flare model overshoot, rotation tracking error, edge-of-data effects, and stitching-boundary residuals); the catalogue is released as a list of transit-like anomalies for community follow-up rather than as individual planet candidates.
2. Single-transit injection-recovery yields 32% recovery at 1000 ppm depth, a regime where the fielded multi-transit classification pipelines (ExoMiner, AstroNet, RAVEN) cannot operate, and where flux-only self-supervised detection had not previously been validated on real photometry.

3. Zero-shot transfer to TESS recovers 47/47 confirmed planets in the PLATO LOPS2 field without retraining, including long-period ( $P > 100$  d) and shallow ( $< 250$  ppm) transits.
4. At PLATO’s 25-second cadence, detection sensitivity reaches 100 ppm, approaching the Earth-analog regime.
5. Conformal prediction provides formal 95% coverage guarantees on candidate rankings, a first in transit detection.

EXOVEL does not replace classification systems, it extends detection to regimes they cannot reach. The complete system is available as a Python package with pretrained weights :

```
pip install exoveil
```

```
from exoveil import ExoVeil
model = ExoVeil.from_pretrained()
```

```
# Detect transits in any Kepler or TESS star
results = model.detect("KIC 11449844")
```

```
# Works with TESS (zero-shot, no retraining)
results = model.detect("TIC 1167538")
```

```
# Or pass custom data
results = model.detect_from_array(time, flux)
```

Each detection returns SNR, estimated depth, and an uncertainty category (*confident*, *data-limited*, *model-uncertain*, or *ambiguous*). Source code, candidate catalogue, and documentation are available at <https://github.com/Pratik25priyanshu20/ExoVeil>.

*Acknowledgements.* I am grateful to Dr. René Heller (Max Planck Institute for Solar System Research) for the careful reading and thoughtful suggestions that shaped this revision. I thank the Kepler and TESS teams for public data access through MAST. P.P. acknowledges support from SRH Hochschule Heidelberg.

## References

- Cadiz-Leyton, M., Cabrera-Vives, G., Protopapas, P., et al. 2025, A&A, 699, A168
- Guerrero, N. M., Seager, S., Huang, C. X., Vanderburg, A., et al. 2021, ApJS, 254, 39
- Hadjigeorghiou, A., Armstrong, D. J., Cui, K., et al. 2025, arXiv e-prints [arXiv:2509.17645], submitted to MNRAS
- Hansen, M. T. & Dittmann, J. A. 2024, AJ, 168, 291
- Hippke, M. & Heller, R. 2019, A&A, 623, A39
- Hones, C. J., Miller, B. K., Heras, A. M., & Foing, B. H. 2021, in NeurIPS 2021 Workshop on Machine Learning and the Physical Sciences
- Islam, M. R. 2026, arXiv e-prints [arXiv:2604.15560]
- Janssen, N., De Ridder, J., Seynaeve, D., et al. 2024, A&A, 681, A18
- Malik, S. A., Eisner, N. L., Mason, I. R., et al. 2025, AJ, 170, 39
- Muthukrishna, D., Mandel, K. S., Lochner, M., Webb, S., & Narayan, G. 2022, MNRAS, 517, 393
- Rauer, H., Aerts, C., Cabrera, J., et al. 2025, Experimental Astronomy, 59, 26
- Salinas, H., Brahm, R., Olmschenk, G., et al. 2025, MNRAS, 538, 2031
- Shallue, C. J. & Vanderburg, A. 2018, AJ, 155, 94
- Singer, N., Williams, J. P., & Ghosh, S. 2025, MNRAS, 539, 1372
- Thompson, S. E., Coughlin, J. L., Hoffman, K., et al. 2018, ApJS, 235, 38
- Valizadegan, H., Martinho, M. J. S., Wilkens, L. S., et al. 2022, ApJ, 926, 120
- Valizadegan, H. et al. 2025, AJ, 170, 287
- Vivien, H. G., Deleuil, M., Janssen, N., et al. 2025, A&A, 694, A293
- Vovk, V., Gammerman, A., & Shafer, G. 2005, Algorithmic Learning in a Random World (New York: Springer)

## Appendix A: Companion gallery of confirmed-planet recoveries

To complement the single-star detection example in Fig. 2, the gallery in Fig. A.1 below presents EXOVEIL’s recovery of four additional confirmed Kepler exoplanets in the blind search, spanning host types from K dwarf to F dwarf and orbital periods from 2.2 to 4.9 days. Each column shows one star with the same three-panel layout as Fig. 2: observed flux with world-model prediction, the prediction residual, and a wide  $\pm 25$  d residual context.

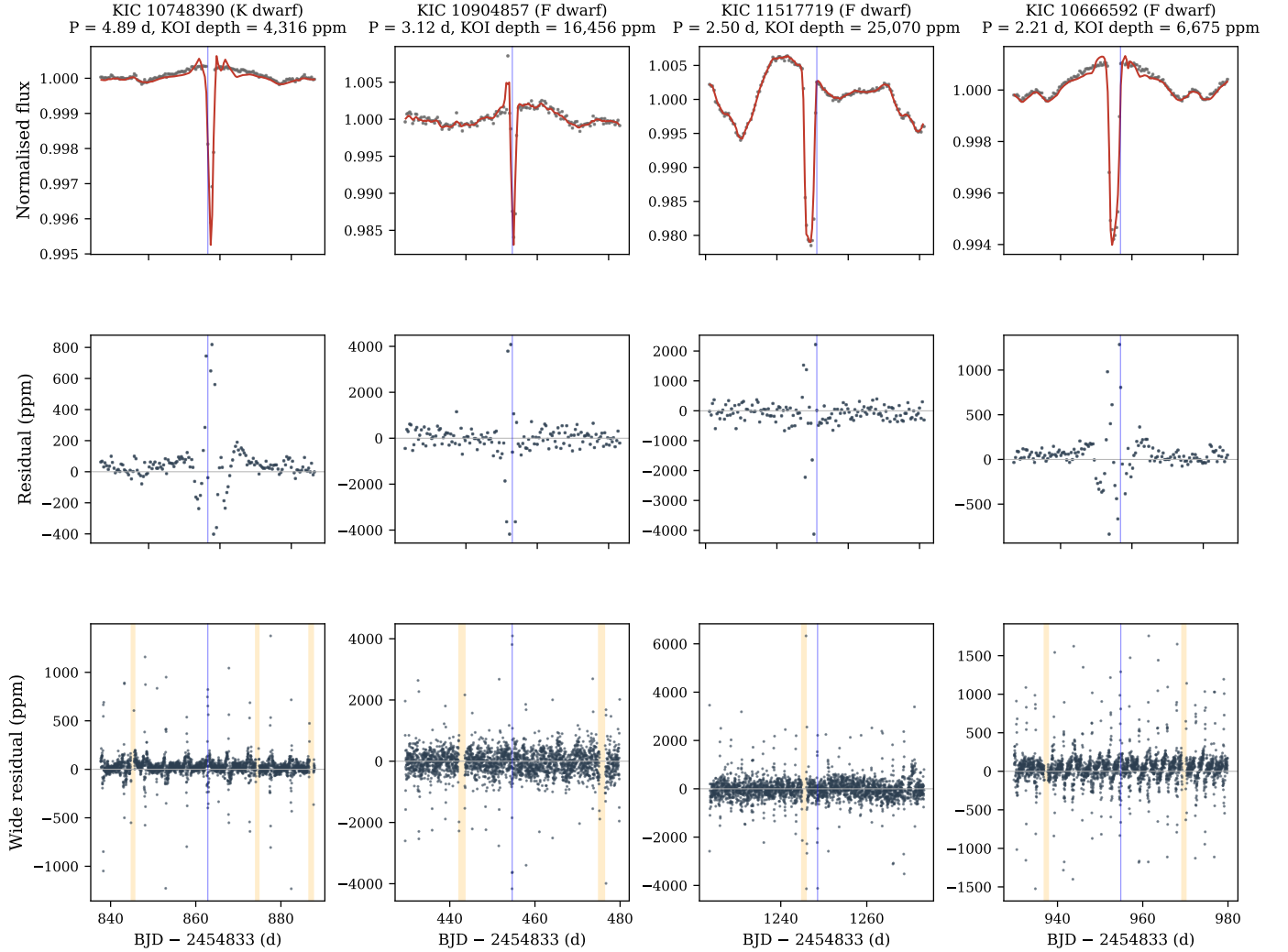


**Fig. A.1.** Four additional confirmed Kepler exoplanets recovered by EXOVEIL in the blind search, complementing the main-text example in Fig. 2. From left: KIC 10748390 (K dwarf,  $T_{\text{eff}} = 4778$  K,  $P = 4.89$  d, KOI depth 4 316 ppm); KIC 10904857 (F dwarf,  $T_{\text{eff}} = 6122$  K,  $P = 3.12$  d, 16 456 ppm); KIC 11517719 (F dwarf,  $T_{\text{eff}} = 6039$  K,  $P = 2.50$  d, 25 070 ppm); KIC 10666592 (F dwarf,  $T_{\text{eff}} = 6440$  K,  $P = 2.21$  d, 6 675 ppm). *Top row:* observed Kepler flux (grey) and world-model prediction (red) around the event. *Middle row:* prediction residual with the event marker. *Bottom row:* wide  $\pm 25$  d residual context, with  $> 0.5$ -day gaps highlighted in orange. Panels are zoomed to  $\pm 1.5$  d for a single-transit view; the wide-view panel confirms periodic recovery and absence of nearby data gaps.